Front. Optoelectron. China 2009, 2(4): 368–378
DOI 10.1007/s12200-009-0026-8

RESEARCH ARTICLE

New progress of mm-wave radio-over-fiber system based on OFM

Rujian LIN (✉), Meiwei ZHU, Zheyun ZHOU, Haoshuo CHEN, Jiajun YE

Key Laboratory of Specialty Fiber Optics and Optical Access Networks, Shanghai University, Shanghai 200072, China

Abstract This paper presents an overview on new progresses of millimeter wave (mm-wave) radio-over-fiber (RoF) system based on mm-wave generation by optical frequency multiplication (OFM), including generation of high-order optical side modes by optical modulation using dual-drive Mach-Zehnder modulator (DD-MZM) and enhancement of high-order optical side mode induced by selective amplification due to stimulated Brillouin scattering (SBS). The paper describes OFM by using DD-MZM in principle and verifies it in an experimental bidirectional 40 GHz RoF system. SBS amplification enhances the generated information-bearing mm-wave in downlink and also helps in producing a pure reference mm-wave for radio frequency-intermediate frequency (RF-IF) down-conversion in uplink. These efforts pushed the OFM technology of mm-RoF systems to achieve more and more feasibility and cost-effectiveness.

Keywords networks, optical communications, radio-over-fiber (RoF) system, optical frequency multiplication (OFM), Mach-Zehnder modulator (MZM), self-heterodyne, stimulated Brillouin scattering (SBS), free spectrum range (FSR), millimeter wave (mm-wave)

1 Introduction

In recent years, radio-over-fiber (RoF) technology, employed especially in millimeter wave (mm-wave) transmission system, has attracted more and more attention due to its characteristics of flexible access, broad bandwidth and immunity to electromagnetic interference. mm-RoF system is the optical fiber links between central station (CS) and base stations (BS). Signal processing is mostly concentrated at CS to make BS just a light wave to mm-wave converter and as simple as possible to ensure the low cost. The key technology of mm-RoF system is the mm-wave generation by optics.

Among the optical techniques for mm-wave generation published by now, such as optical heterodyning of two laser beams or two laser modes [1–6], self-heterodyning of side modes generated by external modulation [7–12], optoelectronic mixing [13,14] and optical frequency multiplication (OFM) [15–17], OFM based on harmonic generation from low-frequency microwave is a promising and cost-effective technique because it does not need any mm-wave oscillator, frequency multiplier or modulator at CS and BS and mm-wave sub-carrier delivered over the fiber link.

A bidirectional mm-RoF system based on OFM using sinusoidal optical phase sweeping and periodic optical filtering has been reported [18]. However, the effectiveness of high harmonics generation relies on the stringent control of laser wavelength and optical filter free spectrum range (FSR) making the system unreliable. In this paper, an even simpler and more cost-effective OFM solution is proposed where the tunable DFB laser and periodic optical filter are cancelled. The new implementation performs the high-order optical side-mode generation and PM-IM conversion in just one $LiNbO_3$ dual-drive Mach-Zehnder modulator (DD-MZM). However, the generation of high-order optical side mode depends on the driving microwave power and optical gain of erbium-doped fiber amplifier (EDFA). To reduce the driving power requirement, a stimulated Brillouin scattering (SBS) amplification to the optical signal can be utilized instead of EDFA amplification. The theoretic analysis, simulation and experiment results are presented.

2 Principle of mm-wave generation by modulation on MZM

In principle, the photonic generation of mm-wave is quite simple. When two coherent laser beams or two optical

Received November 20, 2008; accepted December 29, 2008

E-mail: rujianlin@vip.sina.com

modes from a laser with a preselected wavelength separation are incident on a photo-detector, the heterodyne process produces an mm-wave output in the photocurrent. This method requires an especially made laser system that employs either two single-mode lasers optically phase locked to each other or a multimode laser with mode-locking caused by mm-wave injection. Therefore, this kind of technique is too expensive to be useful.

A simple way to generate two coherent optical modes is a laser beam intensity modulated in an external modulator. When a continuous light wave passes through a $LiNbO_3$ DD-MZM driven by an RF signal at angular frequency ω_s, as shown in Fig. 1, the optical spectrum of the output light wave has one or two side modes around the central angular frequency ω_0 of the light source depending on the phase difference between the RF signals and the direct current (DC) bias on two arms of DD-MZM. After propagating over an optical fiber, the central carrier and single side mode or the two side modes with carrier suppressed can induce a pure mm-wave at frequency ω_s or $2\omega_s$ by self-heterodyne in a photodiode, where the same laser phase noise in the two modes is cancelled out. In addition, although the phase of generated mm-wave varies with the fiber length due to fiber dispersion, its amplitude does not fade, so this is a fiber dispersion tolerable method for mm-wave generation. The disadvantage of this technique is the demand of an mm-wave source at CS. The disadvantage of this modulation method is the utilization of mm-wave generator in CS, which is not cost-effective.

The most cost-effective approach to photonic generation of mm-wave is optical frequency multiplication (OFM). Figure 2 shows a basic arrangement of OFM. In CS, a light wave launched by a distributed feedback laser diode (DFB-LD) is first phase modulated in an optical phase modulator by an RF signal at frequency f_s with a large modulation index. The output light wave from the phase modulator has a lot of side modes separated by f_s, as shown in Fig. 3. This phase spectrum is converted into an intensity spectrum by passing the phase-modulated light wave through a periodic optical filter (Mach-Zehnder interferometer), as shown in Fig. 4. These intensity side modes beat each other in the photodetector (PD) at BS, producing a series of harmonics of the RF signal, as shown in Fig. 5. In this way, an mm-wave at frequency nf_s is generated, which can be picked up using a narrowband band-pass filter and amplified for radiating into the air via an antenna.

The electric field at the output of optical phase modulator is expressed as

$$E_i(t) = E_c \exp[\,j\omega_c t + j\beta \sin(\omega_s t)], \tag{1}$$

where E_c is the amplitude of electric field, ω_c is the central angular frequency of optical source, ω_s is the angular frequency of phase sweeping signal and β is the phase modulation index. After passing through the MZ

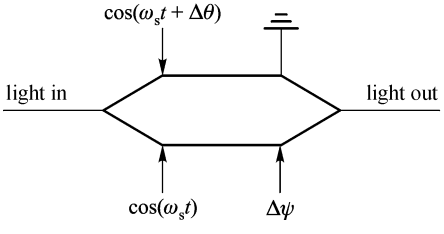

(a)

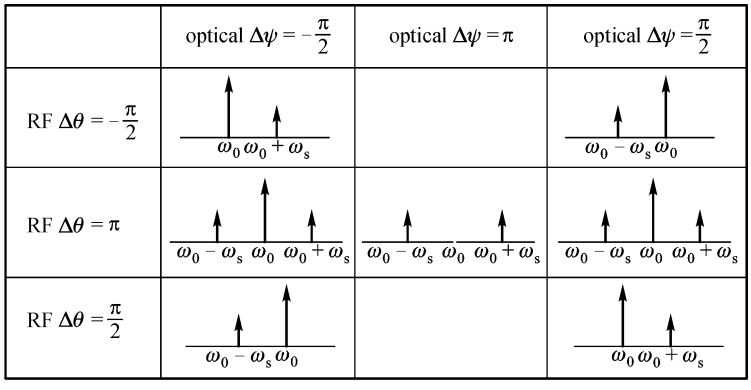

(b)

Fig. 1 RF-driven DD-MZM

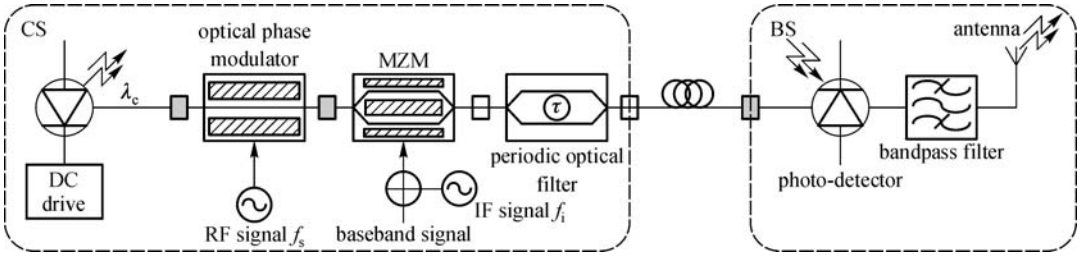

Fig. 2 Basic configuration of OFM

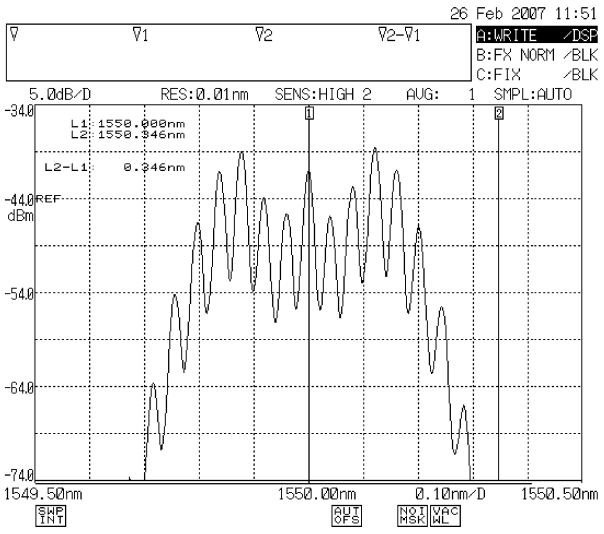

Fig. 3 Light wave spectrum after phase modulation

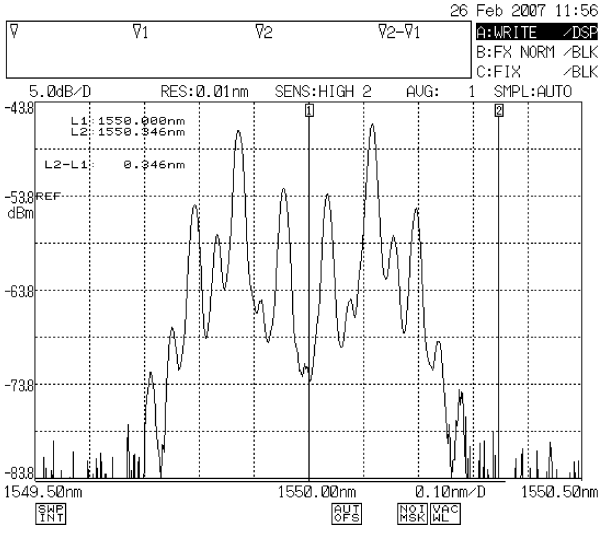

Fig. 4 Light wave spectrum after phase-intensity conversion

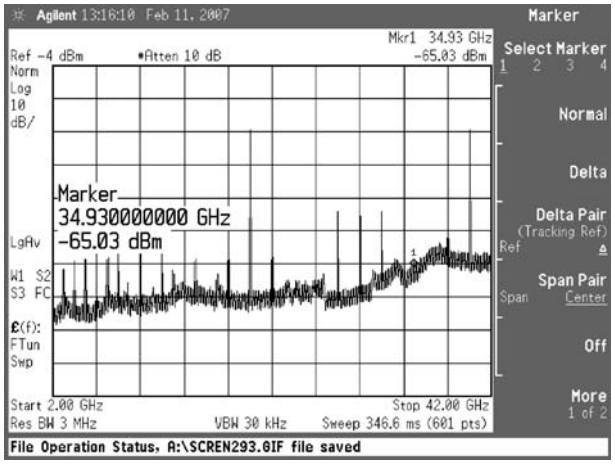

Fig. 5 Photocurrent spectrum after self-heterodyning

interferometer with delay parameter τ, the electric field becomes

$$E_o(t) = E_c \exp[j\omega_c t + j\beta \sin(\omega_s t)] + E_c \exp[j\omega_c (t-\tau) + j\beta \sin(\omega_s (t-\tau))]. \quad (2)$$

The photocurrent is proportional to $E_o(t)E_o^*(t)$, i.e.,

$$\begin{aligned} i_d(t) &= \frac{1}{2}R[E_o(t)E_o^*(t)] \\ &= \frac{1}{2}RE_c^2(t)\left\{1+\cos\left[\omega_c\tau + 2\beta\sin\frac{\omega_s\tau}{2}\cdot\cos\left(\omega_s t - \frac{\omega_s\tau}{2}\right)\right]\right\} \\ &= \frac{1}{2}RE_c^2(t)\left\{\cos(\omega_c\tau)\left[J_0\left(2\beta\sin\frac{\omega_s\tau}{2}\right) + 2\sum_{n=1}^{\infty}J_{2n}\left(2\beta\sin\frac{\omega_s\tau}{2}\right)\cdot\cos(2n\omega_s t - n\omega_s\tau)\right] - \sin(\omega_c\tau)\cdot\left[2\sum_{n=1}^{\infty}J_{2n-1}\left(2\beta\sin\frac{\omega_s\tau}{2}\right)\cdot\cos\left((2n-1)\omega_s t - \frac{2n-1}{2}\omega_s\tau\right)\right]\right\}, \end{aligned} \quad (3)$$

where R is a proportional constant related to the responsivity of PD and $J_n(x)$ is the nth Bessel function of x. From Eq. (3), it is revealed that if $\omega_c\tau = k\pi$ (k is integer) and $\omega_s\tau = \pi$, each of even harmonics in the photocurrent approaches its maximum values, while all odd harmonics disappear, i.e.,

$$i_d(t) = \frac{1}{2}RE_c^2(t)\left[J_0(2\beta) + 2\sum_{n=1}^{\infty}(-1)^n J_{2n}(2\beta)\cos(2n\omega_s t)\right]. \quad (4)$$

This means that the central wavelength λ_c of laser source and the delay constant τ of MZ interferometer should be kept to meet a specific relation; otherwise, the mm-wave generation will not be effective. For example, the parameters of system in Fig. 2 have been taken as: f_s = 5 GHz, τ = 0.1 ns, and $\lambda_c = 2c\tau/k$, where c is the light velocity in vacuum. If k = 38706, 38707 and 38708, then λ_c = 1550.147, 1550.107 and 1550.067 nm, respectively. This means that λ_c deviates from its optimum value by 0.02 nm, corresponding to frequency deviation by 2.5 MHz, will cause the amplitude of desired harmonic varying from the maximum to zero. Hence, this kind of OFM configuration for mm-wave generation is found non-stable.

Furthermore, the trouble in the real situation is the

temperature dependence of τ. If one wants the system stable, the MZ interferometer should be temperature stabilized in addition to that the laser should be wavelength tunable. Hence, this kind of OFM configuration for mm-wave generation is not cost-effective.

Nevertheless, OFM technique is simpler and less expensive than other techniques for photonic generation of mm-wave, because it does not need any millimeter oscillator and up-conversion chain both at CS and at BS. The task of researchers is to find a new OFM implementation to make the system more stable and even more cost-effective.

3 Novel mm-wave radio-over-fiber system based on OFM using DD-MZM

Recognize that there are two basic processes for OFM: optical phase modulation with large modulation index to generate high-order optical side modes and phase modulation-to-intensity modulation conversion to make self-heterodyne happen in PD. For the implementation of phase modulation-to-intensity modulation conversion, it is necessary to have two laser beams interfering with each other, but MZ filter is not the only device being able to make optical interference.

Actually, DD-MZM is a parallel combination of two optical phase modulators and its two arms can make optical interference happen. Therefore, a two-way 40 GHz RoF system based on high-order optical side-mode generation and self-heterodyne using a DD-MZM can be configured as Fig. 6.

In downstream, a 1550 nm polarization-adjusted laser beam in CS is injected into a DD-MZM, whose two arms are DC-biased and RF-driven separately. Two 5 GHz sinusoidal waves with phase difference π are driving the DD-MZM to carry out optical phase modulation with a large index in each arm. At the combining point of DD-MZM, the two optical beams with different phases interfere with each other, converting optical phase modulation into optical intensity modulation with many high-order side modes. These optical modes are re-modulated in another intensity modulator (IM) by an information-bearing 2 GHz intermediate frequency (IF) signal and then transmitted over a downlink fiber of 20 km. Finally, they beat at PD in BS, generating many electrical harmonics of 5 GHz signal, among which any harmonic can be picked up by a specific narrowband band-pass filter. In this way, not only a pure 40 GHz signal but also a 38 GHz mm-wave carrying 2×100 Mbps Ethernet data in binary phase shift keying (BPSK) format are generated. The latter will be amplified and radiated to the air via an antenna. In upstream, the 38 GHz signal from the antenna is amplified by low noise amplifier (LNA) and then mixed with the amplified local 40 GHz signal, resulting in a 2 GHz IF signal. The filtered and amplified IF signal directly modulates a DFB-LD, being sent back to CS via the uplink fiber and recovered at PD. Eventually, the amplified IF signal is BPSK demodulated into 2× 100 Mbps Ethernet data.

The theoretic analysis on mm-wave generation in Fig. 6 is shown below.

Assuming E_1 and E_2, the amplitude of electric field input to two arms of DD-MZM; τ, the time delay difference between two arms of DD-MZM; θ, the phase difference between two 5 GHz sweep signals; $\Delta\varphi_{dc}$, the initial phase difference of light waves in the two arms of DD-MZM determined by the bias voltages; β_1 and β_2, the phase modulation index caused by the two sweep signals, respectively; ω_c and ω_s, the angular frequency of the light wave and the sweep signal, respectively; and $\varphi_N(t+\tau)$ and $\varphi_N(t)$, the laser phase noise in two arms of DD-MZM, the electrical field of output light wave from DD-MZM is

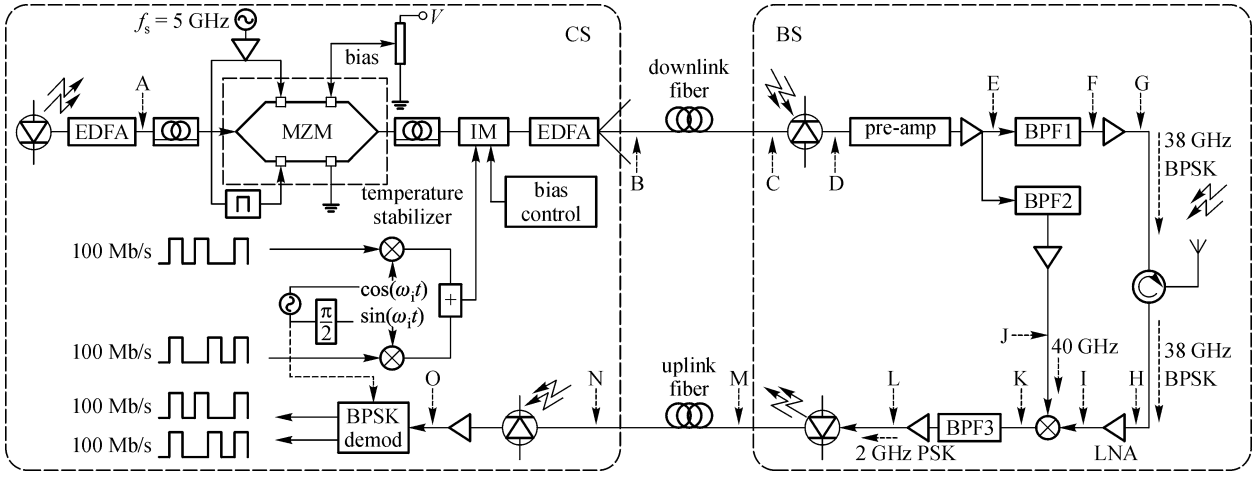

Fig. 6 Bidirectional 38/40 GHz RoF system based on OFM using dual-electrode MZM (demod: demodulator; pre-amp: pre-amplifier)

$$E_o = E_1\exp[j\omega_c(t+\tau) + j\beta_1\cos(\omega_s(t+\tau)+\theta) + \Delta\varphi_{dc} + \varphi_N(t+\tau)] + E_2\exp[j\omega_c t + j\beta_2\cos(\omega_s t) + \varphi_N(t)]. \quad (5)$$

The photocurrent $i_d(t)$ in PD produced by light wave injection is

$$i_d(t) \propto E_o E_o^* = E_1^2 + E_2^2 + 2E_1E_2\cos[\beta_1\cos(\omega_s t + \omega_s\tau + \theta) - \beta_2\cos(\omega_s t) + \omega_c\tau + \Delta\varphi_{dc} + \varphi_N(t+\tau) - \varphi_N(t)].$$

Setting $\Delta\varphi = \omega_c\tau + \Delta\varphi_{dc}$ and $\alpha = \omega_s\tau + \theta$, $i_d(t)$ can be simplified as

$$\begin{aligned} i_d(t) &= \frac{1}{2}R\{E_1^2 + E_2^2 + 2E_1E_2\cos[\beta_1\cos(\omega_s t + \alpha) - \beta_2\cos(\omega_s t) + \Delta\varphi + \varphi_N(t+\tau) - \varphi_N(t)]\} \\ &= \frac{1}{2}R\{E_1^2 + E_2^2 + 2E_1E_2\cos[\beta_1\cos\alpha\cos(\omega_s t) - \beta_1\sin\alpha\sin(\omega_s t) - \beta_2\cos(\omega_s t) + \Delta\varphi + \varphi_N(t+\tau) - \varphi_N(t)]\} \\ &= \frac{1}{2}R(E_1^2 + E_2^2) + RE_1E_2\{\cos[\Delta\varphi + \varphi_N(t+\tau) - \varphi_N(t)]\cos[\beta_{12}\cos(\omega_s t + \phi)] \\ &\quad - \sin[\Delta\varphi + \varphi_N(t+\tau) - \varphi_N(t)]\cdot\sin[\beta_{12}\cos(\omega_s t + \phi)]\}, \end{aligned} \quad (6)$$

where $\beta_{12} = [(\beta_1\cos\alpha - \beta_2)^2 + (\beta_1\sin\alpha)^2]^{1/2}$, and $\phi = \tan^{-1}[-\beta_1\sin\alpha/(\beta_1\cos\alpha - \beta_2)]$. In a DD-MZM, the two arms are identical in length; therefore, $\tau = 0$, the laser phase noise terms in photocurrent, is cancelled with each other. In addition, if $\alpha = \omega_s\tau + \theta = 180°$ holds, β_{12} reaches its maximum value $\beta_1 + \beta_2$ and $\phi = 0$. Expanding $i_d(t)$ into a series by using Bessel function gives

$$i_d(t) = \frac{1}{2}R(E_1^2 + E_2^2) + RE_1E_2\left\{\cos\Delta\varphi\left[J_0(\beta_{12}) + 2\sum_{n=1}^{\infty}(-1)^n J_{2n}(\beta_{12})\cdot\cos(2n\omega_s t)\right] + \sin\Delta\varphi\left[2\sum_{n=1}^{\infty}(-1)^n J_{2n-1}(\beta_{12})\cdot\cos((2n-1)\omega_s t)\right]\right\}. \quad (7)$$

The photocurrent is composed of a lot of even- and odd-order harmonics of the sweep signal. By adjusting the bias voltage V_{dc} to make $\Delta\varphi = \omega_c\tau + \Delta\varphi_{dc} = \pi V_{dc}/V_\pi = k\pi$, $k = 0,1,2,\ldots$, $\cos\Delta\varphi = \pm 1$ and $\sin\Delta\varphi = 0$, all the odd-order harmonics disappear, while each even-order harmonic reaches its maximum:

$$i_d(t) = \frac{1}{2}R(E_1^2 + E_2^2) + R\left[E_1E_2J_0(\beta_1 + \beta_2) \pm 4E_1E_2\sum_{n=1}^{\infty}J_{2n}(\beta_1 + \beta_2)\cos(2n\omega_s t)\right]. \quad (8)$$

If a specific value of $\beta_1 + \beta_2$ is taken, the specific order Bessel function reaches its maximum. For example, to generate 40 GHz carrier from 5 GHz signal (multiplying factor is 8), setting $\beta_1 = \beta_2 = 4.8$ gives $J_8(9.6) = 0.3244$.

To carry the baseband information on the mm-wave, an IM is driven by a 2 GHz IF microwave, which is BPSK modulated by the baseband signal in advance. The electrical field of intensity-modulated light wave is represented as Eq. (1) multiplied by $[1 + k_a m(t)]^{1/2}$, where k_a is the optical intensity modulation index; $m(t)$ is the sum of two orthogonal BPSK signals:

$$m(t) = \cos(\omega_i t + \phi_I) + \sin(\omega_i t + \phi_Q),$$

where ω_i is the IF angular frequency, ϕ_I is the in-phase symbol, and ϕ_Q is the quadrature phase symbol. The photocurrent becomes

$$\begin{aligned} i_d(t) = \frac{1}{2}R\Bigg\{ & [1 + k_a m(t)][E_1^2 + E_2^2 + 2E_1E_2J_0(\beta_1 + \beta_2)] \\ & \pm 2RE_1E_2\sum_{n=1}^{\infty}J_{2n}(\beta_1 + \beta_2)\cos(2n\omega_s t) \\ & \pm Rk_aE_1E_2\Bigg\{\sum_{n=1}^{\infty}J_{2n}(\beta_1 + \beta_2)\cos[(2n\omega_s + \omega_i)t + \phi_I] \\ & + \sum_{n=1}^{\infty}J_{2n}(\beta_1 + \beta_2)\cos[(2n\omega_s - \omega_i)t - \phi_I]\Bigg\} \\ & \pm Rk_aE_1E_2\Bigg\{\sum_{n=1}^{\infty}J_{2n}(\beta_1 + \beta_2)\sin[(2n\omega_s + \omega_i)t + \phi_Q] \\ & + \sum_{n=1}^{\infty}J_{2n}(\beta_1 + \beta_2)\sin[(2n\omega_s - \omega_i)t - \phi_Q]\Bigg\}\Bigg\}. \end{aligned} \quad (9)$$

Take $n = 4$, the second term is 40 GHz pure signal, while the third and fourth terms are 38 and 42 GHz BPSK signal carrying in-phase data; the fifth and sixth terms are 38 and 42 GHz BPSK signal carrying quadrature data.

4 Experiment results of OFM using DD-MZM

First, the optical spectrum of CS output is checked. Figures 7 and 8 show the optical spectrum expansion as the optical phase modulation index increases in case that one arm of DD-MZM is driven. When the 5 GHz driving

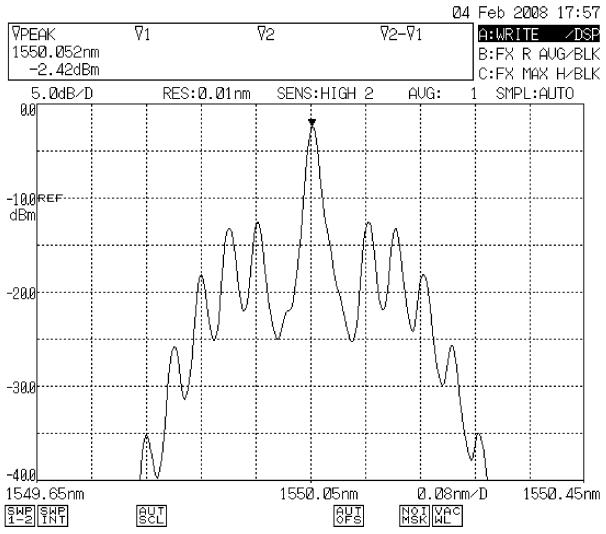

Fig. 7 Optical spectrum for single arm of MZM driven by + 24 dBm

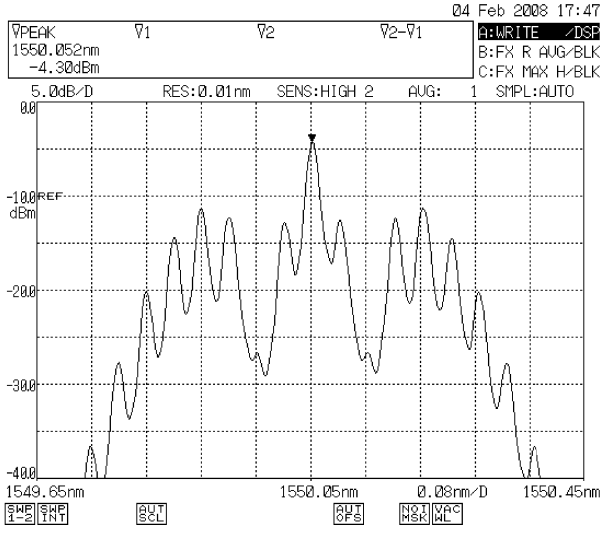

Fig. 8 Optical spectrum for single arm of MZM driven by + 27 dBm

power approaches to + 27 dBm, the ±4th modes rise to the highest, indicating $\beta = 4.8$, as shown in Fig. 8. Applying this best driving power to both arms of DD-MZM, the optical spectrum shown in Fig. 9 becomes a carrier suppressed type with strong side modes around ±20 GHz. It is expected that strong 40 GHz mm-wave will be generated at PD in BS, which is proven by the spectrum at PD output, as shown in Fig. 10, where the 40 GHz peak is the highest among other harmonics and odd harmonics disappear, because the bias voltage has been adjusted to meet $\Delta\varphi = \pi$. To maintain this optimum operating condition, the DD-MZM has been put in a temperature stabilizer.

When the BPSK-modulated 2 GHz IF signal is turned

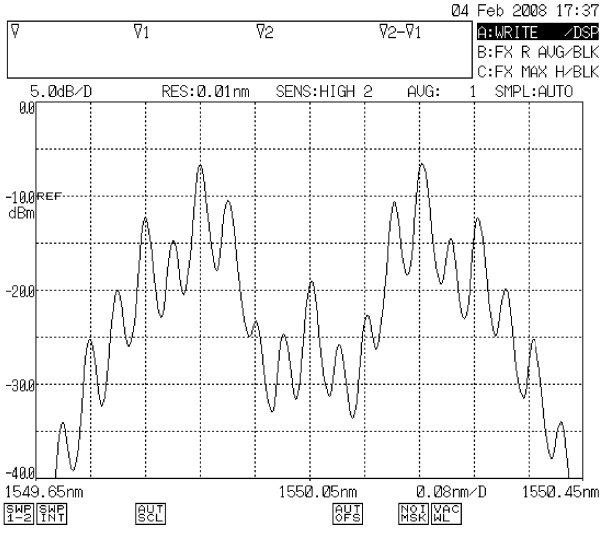

Fig. 9 Optical spectrum for dual arms of MZM driven by + 27 dBm

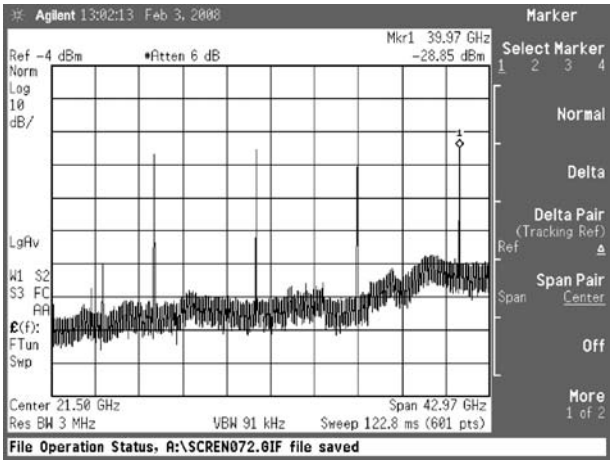

Fig. 10 Spectrum of PD output at point C

on, its spectrum appears around each generated harmonic, as shown in Fig. 11. Figure 12 shows the spectrum of 38 GHz BPSK signal at point D in Fig. 6. The filtered 40 GHz signal is amplified above + 10 dBm with carrier-noise-ratio larger than 50 dB, as shown in Fig. 13, and is good as a local signal for the mixer. The 2 GHz BPSK signal from the mixer is amplified, transmitted over the uplink fiber and recovered in CS, as shown in Fig. 14. Figure 15 shows the BPSK-demodulated 100 Mbps Ethernet data (upper trace) compared with the launched data (lower trace), giving the evidence that the proposed bidirectional 40 GHz RoF system is successful.

It is proven that the OFM technique based on DD-MZM has the following advantages over the phase modulator plus MZ interferometer solution:

1) The optimum condition to make odd harmonics disappear and even harmonics maximum is independent of

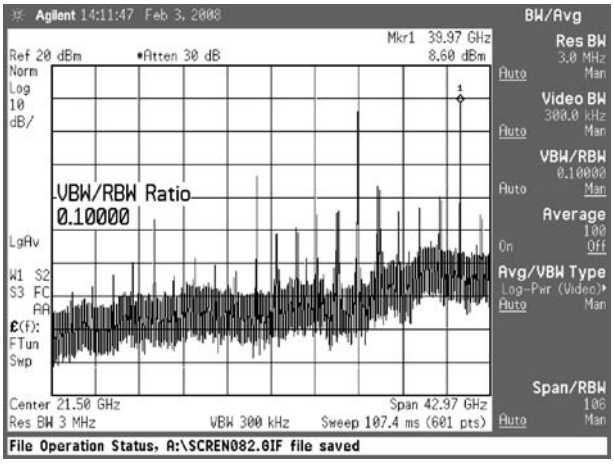

Fig. 11 Spectrum of receiver output at point D

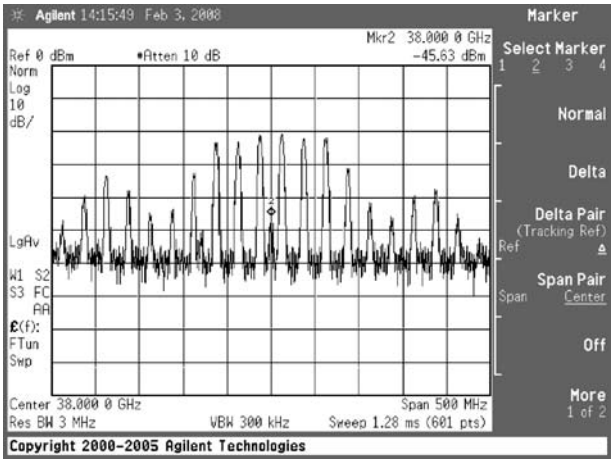

Fig. 12 Spectrum of 38 GHz BPSK at point D

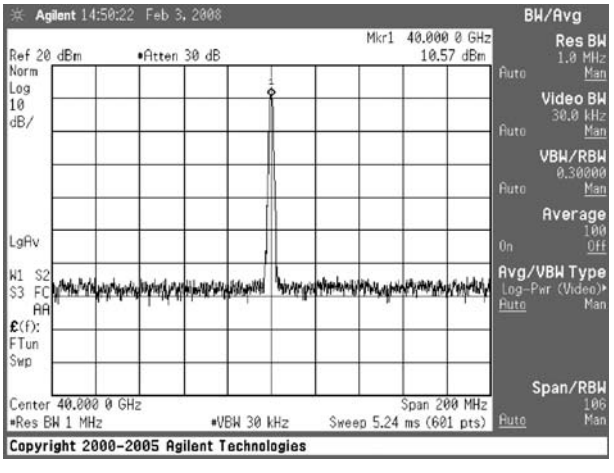

Fig. 13 Spectrum of 40 GHz signal at point E

the laser wavelength, so that the tunable laser is not necessary.

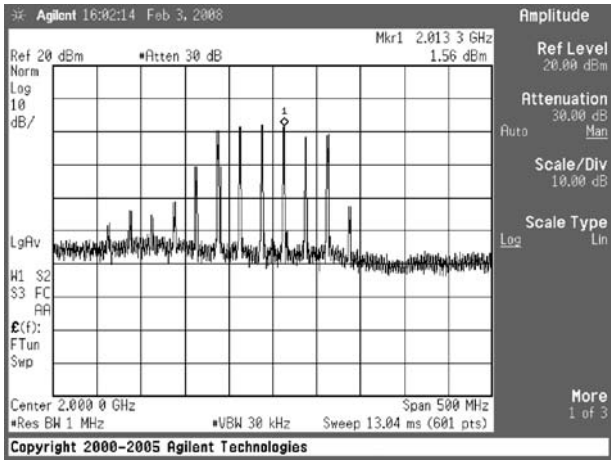

Fig. 14 Spectrum of 2 GHz BPSK at point I

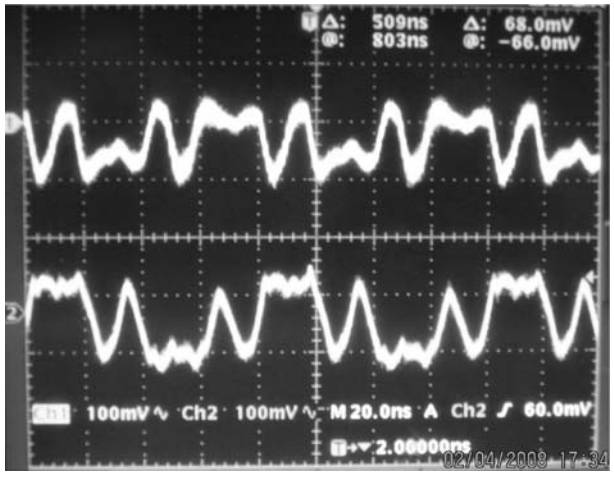

Fig. 15 Waveform of output 100 Mbps data

2) The system no longer needs any periodic optical filter, such as MZ interferometer, to implement PM-IM conversion, so that the system stability is improved by getting rid of temperature-sensitive devices.

3) Laser phase noise is cancelled out, so that output spectrum is purified.

4) Cost-saving is reached by excluding the tunable DFB laser and the MZ interferometer.

5 mm-wave generation by OFM with Brillouin selective amplification

A DD-MZM is used as high-order optical side-mode generator. The light wave launched from an optical source is modulated in the DD-MZM with two different RF signals at the same time on its two RF arms. As shown in Fig. 16, one arm is applied with a microwave signal at the frequency f_s and another one with a PSK-modulated signal at the frequency f_{IF}. The two arms are properly DC-biased.

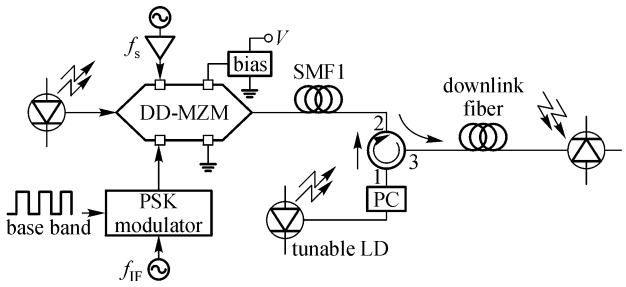

Fig. 16 Diagram of modulation scheme (PC: polarization controller)

In addition, a selective optical amplification based on stimulated Brillouin scattering (SBS) is integrated into OFM scheme making it frequency-agile.

Brillouin selective amplification has been proposed for RoF system [19–21], but the schemes can only produce 11 GHz microwave output due to the limit of Stokes frequency shift. In Ref. [21], Brillouin amplification is imposed on a high-order optical side mode to enhance the mm-wave generation by OFM. Brillouin amplification is also helpful in generating a local reference mm-wave at BS for uplink down-conversion.

The output optical signal from DD-MZM can be described by

$$\begin{aligned} E_{\text{out}}(t) &= E_{\text{c}}\exp[\text{j}\omega_{\text{c}}t + \text{j}\beta\cos(\omega_{\text{s}}t) + \text{j}\phi_{\text{PN}}(t)] \\ &\quad + E_{\text{c}}\exp[\text{j}\omega_{\text{c}}t + \text{j}\alpha\cos(\omega_{\text{IF}}t + \phi_M) \\ &\quad + \text{j}\phi_{\text{PN}}(t)], \end{aligned} \tag{10}$$

where ω_{c} is the angular frequency of the optical carrier; ω_{s} and ω_{IF} are the angular frequencies of RF signal and IF signal, respectively; β and α are the optical phase modulation indexes: $\beta = \pi V_{\text{s}}/V_\pi$, V_{s} is the amplitude of RF signal, V_π is the voltage for π phase shift of MZM; $\alpha = \pi V_{\text{IF}}/V_\pi$, V_{IF} is the amplitude of the PSK IF signal; ϕ_M represents two possible phases 0 and π that convey the baseband data "0" and "1", and $\phi_{\text{PN}}(t)$ is the laser phase noise.

When the output optical signal from the modulator propagates over the fiber SMF1, which is backward pumped by a tunable laser, a certain spectral component of the optical signal is enhanced by SBS amplification caused by the Stokes wave with a spectrum overlapping the optical signal, as shown in Fig. 17. After propagating over the downlink fiber, the electric field of optical signal input to the photodiode can be described in Bessel expansion as

$$\begin{aligned} &E_{\text{out\_amp}}(t) \\ &= E_{\text{c}}\Big\{J_0(\beta)\exp[\text{j}\omega_{\text{c}}t + \text{j}\phi_{\text{PN}}(t)] \\ &\quad + \sum_{m=1}^{\infty}(-1)^m J_{2m}(\beta)\exp[\text{j}\omega_{\text{c}}t + \text{j}2m\omega_{\text{s}}t + \text{j}\phi_{\text{PN}}(t)] \\ &\quad + \sum_{m=1}^{\infty}(-1)^m J_{2m}(\beta)\exp[\text{j}\omega_{\text{c}}t - \text{j}2m\omega_{\text{s}}t + \text{j}\phi_{\text{PN}}(t)] \\ &\quad + \delta(-1)^M J_{2M-1}(\beta)\exp\Big[\text{j}\omega_{\text{c}}t + \text{j}(2M-1)\omega_{\text{s}}t \\ &\quad + \text{j}\phi_{\text{PN}}(t) - \text{j}\frac{\pi}{2}\Big] + \sum_{\substack{m=1 \\ m\neq M}}^{\infty}(-1)^m J_{2m-1}(\beta) \\ &\quad \cdot\exp\Big[\text{j}\omega_{\text{c}}t + \text{j}(2m-1)\omega_{\text{s}}t + \text{j}\phi_{\text{PN}}(t) - \text{j}\frac{\pi}{2}\Big] \\ &\quad + (-1)^M J_{2M-1}(\beta)\exp\Big[\text{j}\omega_{\text{c}}t - \text{j}(2M-1)\omega_{\text{s}}t \\ &\quad + \text{j}\phi_{\text{PN}}(t) - \text{j}\frac{\pi}{2}\Big] + \sum_{\substack{m=1 \\ m\neq M}}^{\infty}(-1)^m J_{2m-1}(\beta) \\ &\quad \cdot\exp\Big[\text{j}\omega_{\text{c}}t - \text{j}(2m-1)\omega_{\text{s}}t + \text{j}\phi_{\text{PN}}(t) - \text{j}\frac{\pi}{2}\Big]\Big\} \\ &\quad + E_{\text{c}}\Big\{J_0(\alpha)\exp[\text{j}\omega_{\text{c}}t + \text{j}\phi_{\text{PN}}(t)] + J_1(\alpha)\exp\Big[\text{j}(\omega_{\text{c}} + \omega_{\text{IF}})t \\ &\quad + \phi_M + \text{j}\phi_{\text{PN}}(t) - \text{j}\frac{\pi}{2}\Big] + J_1(\alpha)\exp\Big[\text{j}(\omega_{\text{c}} - \omega_{\text{IF}})t + \phi_M \\ &\quad + \text{j}\phi_{\text{PN}}(t) - \text{j}\frac{\pi}{2}\Big]\Big\}, \end{aligned} \tag{11}$$

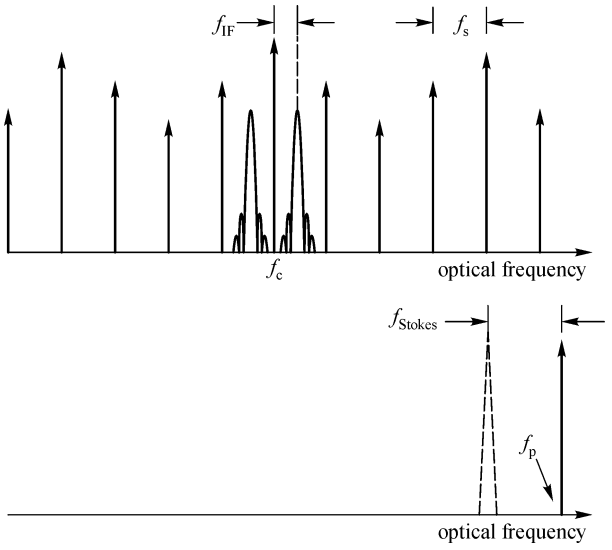

Fig. 17 Stokes spectrum of SBS over optical sideband

where δ is SBS gain coefficient and $f_{\text{c}} + (2M-1)f_{\text{s}}$ is the optical side-mode frequency overlapped by the SBS spectrum. To carry the BPSK-modulated IF signal without phase distortion, the optical modulation index of IF signal is kept low enough, so that the second- and higher-order sideband of light wave caused by the IF signal are omitted, as shown in Eq. (11).

In the photo-detector, the electric field components beat

each other, generating a lot of RF current components at different frequencies, among which two specific components at frequency $(2M-1)f_s$ are

$$i_{2M-1}(t) = \frac{1}{2}R(\delta-1)[J_0(\beta)+J_0(\alpha)] \cdot(-1)^M J_{2M-1}(\beta)\sin[(2M-1)\omega_s t], \quad (12)$$

$$i_{2M-1\_side}(t) = \frac{1}{2}R\delta(-1)^M J_{2M-1}(\beta)J_1(\alpha)\cos[(2M-1)\omega_s t \pm \omega_{IF}t-\phi_M], \quad (13)$$

where R is the proportional coefficient related to fiber attenuation, core area and responsivity of photodiode.

If $f_s = 6$ GHz, $f_{IF} = 2.4$ GHz and $M = 4$ are taken, an mm-wave carrier at 42 GHz and BPSK sidebands at ± 2.4 GHz are obtained from Eqs. (12) and (13):

$$i_7(t) = \frac{1}{2}R(\delta-1)[J_0(\beta)+J_0(\alpha)] \cdot J_7(\beta)\sin[2\pi(7\cdot 6)t], \quad (14)$$

$$i_{7\_side}(t) = \frac{1}{2}R\delta J_7(\beta)J_1(\alpha)\cos[2\pi(42\pm 2.4)t-\phi_M]. \quad (15)$$

The RF spectrum of photo-current output is shown in Fig. 18. It is recognized from Eq. (14) that Brillouin gain coefficient δ determines the existence of odd-order central carrier. If $\delta = 1$, the odd-order central carrier will disappear. The pure central carrier is useful as a local reference necessary for down-converting 39.6 GHz BPSK signal into 2.4 GHz BPSK signal.

To maximize the amplitude of generated mm-wave, the optical modulation indexes α and β should be properly chosen. To control the second- and higher-order sideband component of light wave caused by IF signal low enough, take $\alpha = 0.9$. The amplitudes of 42 GHz carrier and 39.6 GHz lower sideband are proportional to $J_7(\beta)$, which has a maximum at $\beta = 8.3$, as shown in Fig. 19, but it

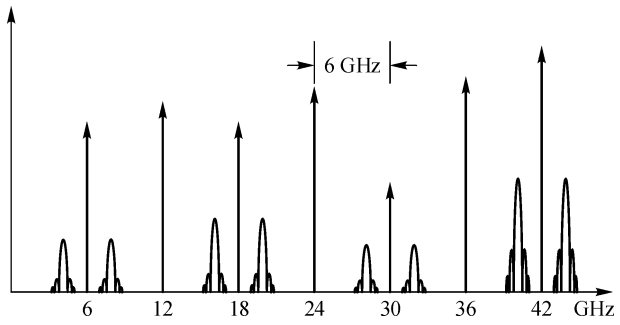

Fig. 18 RF spectrum of photocurrent

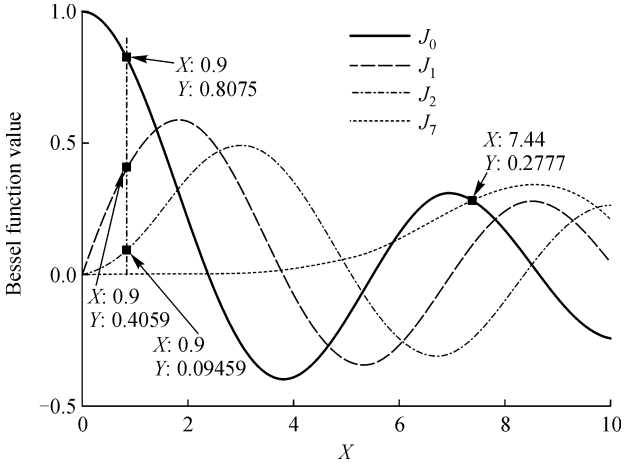

Fig. 19 Curves of Bessel functions

is difficult to implement such a high optical phase modulation index due to the limitation on the output level of 6 GHz signal generator. Therefore, $\beta = 7.44$ has been taken as a compromise parameter between the level of mm-wave and the system feasibility.

An experimental system setup is shown in Fig. 20. The optical source working at wavelength 1550.12 nm (193.5334 THz) has output power of 16 dBm. The dual-electrode MZM with $V_\pi = 4$ V is driven by a 6 GHz RF

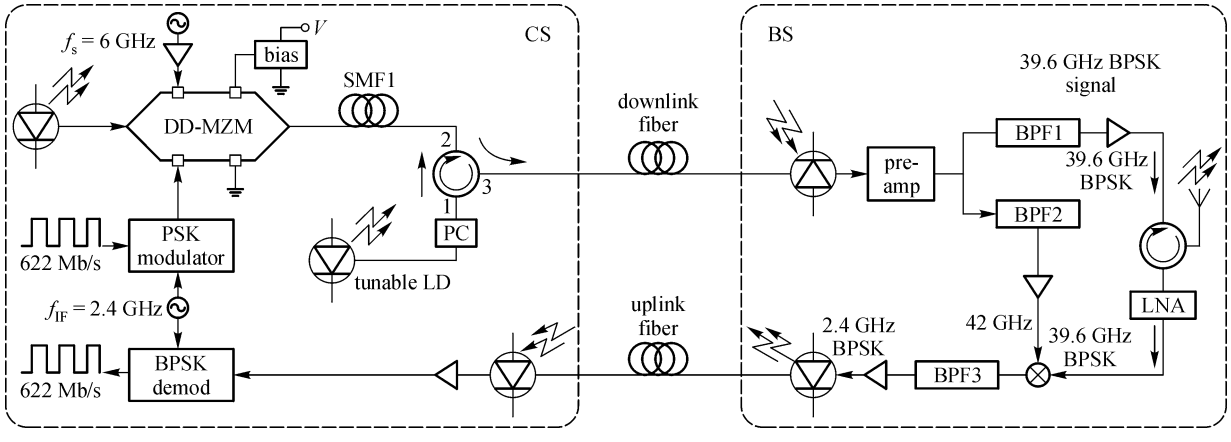

Fig. 20 Bidirectional RoF system setup

signal and a PSK-modulated 2.4 GHz IF signal. To achieve $\beta = 7.44$ and $\alpha = 0.9$, the driving power of RF signal needs to be 29.53 dBm and that of IF signal is 11.18 dBm.

The pump wavelength from the tunable LD is tuned at 1549.70 nm (193.5864 THz), and its power is 20 mW, which creates a Brillouin gain spectrum centered at 1549.78 nm (193.5754 THz), i.e., 11 GHz lower than the pump frequency in 10 km conventional single-mode fiber SMF1. The spectrum of modulated optical signal is shown in Fig. 21, whose 7th sideband is overlapped by the Brillouin gain spectrum and is amplified by 30 dB due to SBS in SMF1.

After transmission over 10 km single-mode fiber, the optical side modes beat at the photodiode in BS. The spectrum of generated mm-wave is shown in Fig. 22, which contains a pure 42 GHz carrier, a 39.6 GHz BPSK signal and a 44.4 GHz BPSK signal. The 42 GHz carrier and the 39.6 GHz BPSK signal are filtered by a narrowband band-pass filter BPF1 and radiated into the air. The 42 GHz carrier behaves as a reference signal for down-converting the 39.6 GHz BPSK signal into the 2.4 GHz BPSK signal in the mobile terminal. The pure 42 GHz carrier is also extracted by another narrowband band-pass filter BPF2 and amplified as the local reference for down-converting the 39.6 GHz BPSK signal received from the antenna. The converted 2.4 GHz BPSK signal is then transmitted by a laser via the uplink fiber back to the central station.

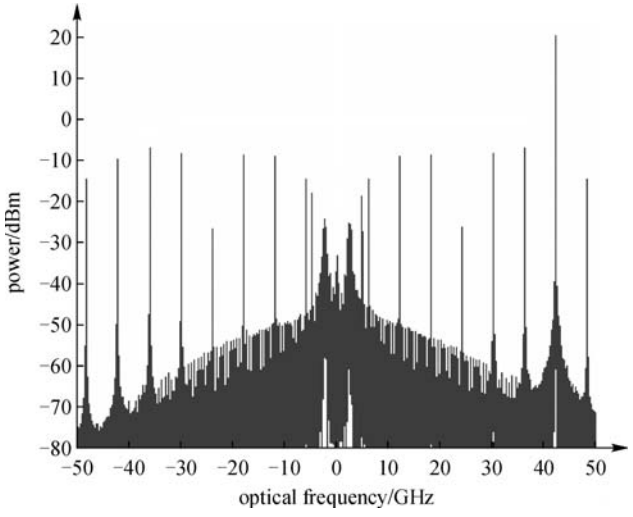

Fig. 21 Optical signal spectrum with the 7th side mode SBS-amplified

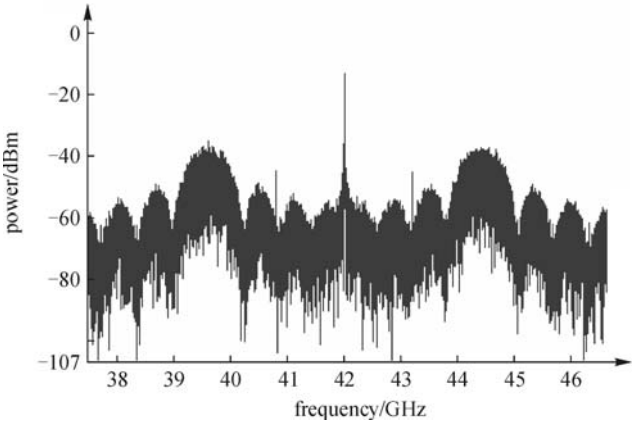

Fig. 22 Spectrum of generated mm-wave by OFM

6 Conclusion

Among the optical techniques used to generate mm-wave for the radio-over-fiber systems, OFM is the most cost-effective one because it converts low-frequency microwave to mm-wave without need for the expensive devices such as mm-wave oscillator and RF-IF multiplication chain both in CS and in BS. To improve the stability of the OFM scheme published by now, this paper exploits DD-MZM as high-order side-mode generator based on which a novel bidirectional 40 GHz RoF system is designed and demonstrated. The system can deliver two 100 Mbps Ethernet data streams over 20 km distance and has many advantages, such as simple, stable in temperature-varying environment, cost-effective without the need for special devices, immune from laser phase noise, bandwidth-expandable in IF schemes and tolerant to fiber dispersion.

In the development of OFM technique, the original optical phase modulator plus MZ interferometer solution has been discarded. Instead, DD-MZM solution has been proven as a more stable and more cost-effective solution. The further improvement in stability can be made by using DFB laser with polarization-maintaining fiber spliced directly to the DD-MZM and by temperature-stabilizing the DD-MZM.

In addition, SBS selective amplification has been employed in RoF systems to enhance the information-bearing mm-wave, to generate a pure reference mm-wave for RF-IF down-conversion, to save an intensity modulator and to make the output frequency tunable.

All these continuous efforts will push the OFM technology of mm-RoF systems to achieve more and more feasibility and cost-effectiveness.

Acknowledgements This work was support by the National Natural Science Foundation of China (Grant No. 60377024) and the Shanghai Leading Academic Discipline Project (No. T0102).

References

1. Gliese U, Neilsen T N, Bruun M, Christensen E L, Stubkjzr K E, Lindgren S, Broberg B. A wideband heterodyne optical

phase-locked loop for generation of 3–18 GHz microwave carriers. IEEE Photonics Technology Letters, 1992, 4(8): 936–938

2. Noel L, Moodie D G, Marcenac D D, Westbrook L D, Nesset D. Novel techniques for high-capacity 60-GHz fiber-radio transmission systems. IEEE Transactions on Microwave Theory and Techniques, 1997, 45(8): 1416–1423
3. Braun R P, Grosskopf G, Rohde D, Schmidt F. Low-phase-noise millimeter-wave generation at 64 GHz and data transmission using optical sideband injection locking. IEEE Photonics Technology Letters, 1998, 10(5): 728–730
4. Ohno T, Sato K, Fukushima S, Doi Y, Matsuoka Y. Application of DBR mode-locked lasers in millimeter-wave fiber-radio system. Journal of Lightwave Technology, 2000, 18(1): 44–49
5. Ogusu M, Inagaki K, Mizuguchi Y, Ohira T. Carrier generation and data transmission on millimeter-wave bands using two-mode locked Fabry-Perot slave lasers. IEEE Transactions on Microwave Theory and Techniques, 2003, 51(2): 382–391
6. Taniguchi T, Sakurai N. An optical/electrical two-step heterodyne for wideband 60 GHz radio-on-fiber access. In: Proceedings of Optical Fiber Communication Conference. 2004, FE1
7. O'Reilly J J, Lane P M, Heidemann R, Hofstetter R. Optical generation of very narrow linewidth millimeter wave signals. Electronics Letters, 1992, 28(25): 2309–2311
8. Schmuck H. Comparison of optical millimeter-wave system concepts with regard to chromatic dispersion. Electronics Letters, 1995, 31(21): 1848–1849
9. Rolf H, Harald S, Rolf H. Dispersion effects in optical millimeter-wave systems using self-heterodyne method for transport and generation. IEEE Transactions on Microwave Theory and Techniques, 1995, 43(9): 2263–2269
10. Gliese U, Norskov S, Nielson T N. Chromatic dispersion in fiber-optic microwave and millimeter-wave links. IEEE Transactions on Microwave Theory and Techniques, 1996, 44(10): 1716–1724
11. Smith G H, Novak D, Ahmed Z. Techniques for optical SSB generation to overcome dispersion penalties in fibre-radio systems. Electronics Letters, 1997, 33(1): 74–75
12. Park J, Sorin W V, Lau K Y. Elimination of the fiber chromatic dispersion penalty on 1550 nm millimeter-wave optical transmission. Electronics Letters, 1997, 33(6): 512–513
13. Kang H S, Choi W Y. CMOS-compatible 60 GHz harmonics optoelectronic mixer. In: Proceedings of IEEE/MTT-S International Microwave Symposium. 2007, 233–236
14. Choi W Y, Kim J Y. Technologies for fiber-fed 60 GHz wireless systems. In: Proceedings of Optical Fiber Communication Conference (OFC). 2007, OWN-1
15. Koonen T, Ng'oma A, Smulders P, Van Den Boom H, Monroy I T, Khoe G D. In-house networks using multimode polymer optical fiber for broadband wireless services. Photonic Network Communications, 2003, 5(2): 177–187
16. Koonen T, Ng'oma A, Larrode M G, Huijskens F, Monroy I T, Khoe G D. Novel cost-efficient techniques for microwave signal delivery in fibre-wireless networks. In: Proceedings of European Conference on Optical Communication. 2004, 120–123
17. Larrode M G, Koonen A M J, Olmos J J V, Verdurmen E J M, Turkiewicz J P. Dispersion tolerant radio-over-fibre transmission of 16 and 64 QAM radio signals at 40 GHz. Electronics Letters, 2006, 42(15): 872–874
18. Xiu M L, Lin R J. Report on 40 GHz-RoF bidirectional transmission experiment system with pilot tone. In: Proceedings of Conference on Lasers and Electro-Optics/Pacific Rim. 2007, 493–494
19. Shen Y C, Zhang X M, Chen K S. Optical single sideband modulation of 11-GHz RoF system using stimulated Brillouin scattering. IEEE Photonics Technology Letters, 2005, 17(6): 1277–1279
20. Park C S, Lee C G, Park C S. Photonic frequency upconversion based on stimulated Brillouin scattering. IEEE Photonics Technology Letters, 2007, 19(10): 777–779
21. Chen H S, Lin R J, Ye J J. A scheme of yielding tunable millimeter-wave based on stimulated Brillouin scattering. In: Proceedings of China-Japan Joint Microwave Conference. 2008, 591–594